

Magnetic resonance and the phase transitions in the two-dimensional antiferromagnet $(\text{NH}_3)_2(\text{CH}_2)_3\text{MnCl}_4$

A. I. Zvyagin, M. I. Kobets, V. N. Krivoruchko, A. A. Stepanov, and D. A. Yablonskii

Physicotechnical Institute of the Academy of Sciences of the Ukrainian SSR, Donetsk

(Submitted 5 July 1985)

Zh. Eksp. Teor. Fiz. **89**, 2298–2317 (December 1985)

An experimental and theoretical study is made of the quasi-two-dimensional antiferromagnet $(\text{NH}_3)_2(\text{CH}_2)_3\text{MnCl}_4$. It is shown that this crystal exhibits a substantially noncollinear (canted) four-sublattice magnetic structure due to the weakness of the interlayer exchange interaction. Two spin-orientation phase transitions ($H_{sf} = 24.6$ kOe, $H_c = 98$ kOe) are detected and studied for magnetic-field orientations along the \mathbf{b} axis of the crystal. It is shown that these transitions have a number of peculiar features. The frequency-field curves of the four branches of the antiferromagnetic resonance and the features of the rf magnetic susceptibility tensor are investigated at frequencies in the range 15–200 GHz and in fields up to 150 kOe. By a comparison of the theoretical calculations with the experimental results the magnetic structure is deciphered and values are found for the effective fields characterizing $(\text{NH}_3)_2(\text{CH}_2)_3\text{MnCl}_4$.

I. INTRODUCTION

The overwhelming majority of antiferromagnets are many-sublattice systems. Nevertheless, many of their properties can be described well in the two-sublattice model. This is true of antiferromagnets whose magnetic structure is collinear in the exchange approximation and in which the exchange interactions are substantially stronger than the relativistic interactions. However, there exists a wide class of low-dimensional magnets in which the interplane (for quasi-two-dimensional magnets) or interchain (for quasi-one-dimensional magnets) exchange H'_e is comparable in magnitude to the relativistic interaction H_A . As we show in this paper, such a circumstance leads to a number of peculiar features in the rf and static properties of these systems. The features of the rf properties of many-sublattice antiferromagnets with low-dimensional magnetic structures are due to the emergence of additional low-lying branches in the AFMR spectrum, while the features of the static properties are due to the intercoupling of the layers (or chains).

It is known that in addition to the acoustic modes of the AFMR, the spectrum of a four-sublattice antiferromagnet should contain optical (or exchange) modes with frequencies comparable to the energy of the exchange interactions of the antiferromagnet. This circumstance was apparently first pointed out by Joenk,¹ who considered the problem of the optical modes in a magnetic structure of the plane cross type—a structure characterized by two antiferromagnetism vectors \mathbf{L} and \mathbf{l} , with $L \gg l$. In such a model the square of the frequency of the optical mode is proportional to the product $H_e^{AF} H_e^F$ of the exchange fields which give rise to the magnetic structure of the system, and the intensity ratio of the lines of the optical and acoustic modes goes as $\sim H_D^2 / H_e^{AF} H_e^F$.

Estimates made for a three-dimensional antiferromagnet on the basis of the expressions obtained in Refs. 2 and 3 explain why most of the properties of three-dimensional antiferromagnets having a large number of sublattices are described well by the two-sublattice model. The most impor-

tant difficulties preventing observation of the optical modes in three-dimensional antiferromagnets in AFMR experiments are: 1) the frequencies of the optical modes of typical antiferromagnets correspond to energies in the exchange region (~ 100 K, submillimeter wavelengths), where, first, until recently there were no high-power radiation sources and, second, there are strong electric-dipole phonon absorption bands; and 2) the intensity of the optical modes is low. Nevertheless, the optical modes have recently been detected^{4,5} in the three-dimensional antiferromagnet $\text{CuCl}_2 \cdot 2\text{H}_2\text{O}$.

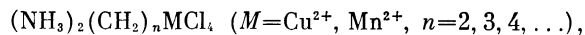
These difficulties do not arise in a study of the optical modes in an antiferromagnet of lower dimensionality. As we show in this paper, the presence of weak exchange interactions in low-dimensional antiferromagnets can bring about a situation in which, first, the frequency of the optical modes is small, comparable to that of the acoustic modes, and second, the intensity of the absorption by the optical modes is large, comparable to that of the absorption by acoustic modes. It is for this reason that the exchange modes in the antiferromagnetic resonance were first detected⁶ in the low-dimensional antiferromagnet $(\text{NH}_3)_2(\text{CH}_2)_3\text{MnCl}_4$.

Because of the decrease in the frequencies and the increase in the intensity of the optical modes of the spin-wave branch, the optical modes take on the same status as the branches of the usual acoustic modes and determine the dynamics and thermodynamics of low-dimensional systems. In other words, the optical modes are an integral and extremely important property of many-sublattice low-dimensional magnets.

The presence of a weak exchange interaction $H'_e \sim H_A$ enhances the role of the relativistic interactions. Then, if the symmetry class of the layers (chains) is lower than the symmetry class of the crystal, the magnetic structure of the system turns out to be substantially noncollinear (a relativistically canted structure). This causes a number of peculiar static properties of low-dimensional magnets. For example, the picture of the spin-reorientation phase transitions, such as the spin-flop transition, changes substantially; at $T = 0$ a

longitudinal susceptibility appears, having a magnitude comparable to the transverse susceptibility; there is a marked increase in the "twisting" susceptibility—an external field imposed along the direction of the weak magnetic moment causes not only a bending of the magnetic moments of the sublattices toward the direction of the field but also a rotation of the moments about the field direction.

Typical representatives of the class of low-dimensional many-sublattice magnets are compounds with the general formula



which are two-dimensional Heisenberg ferromagnets and antiferromagnets. The structure of these crystals is made up of practically square layers of magnetic ions in an octahedral chlorine environment, with long alkyl-ammonium groups between them. The small value of the superexchange on account of the large distance between spins on neighboring layers leads to a quasi-two-dimensional behavior of these systems. The possibility of changing the number of methylene groups in these compounds makes it possible to change the degree of their magnetic two-dimensionality over very wide limits. According to the experiments of several authors⁷ the ratio of the interlayer to intralayer exchange interactions can be of the order of 10^{-8} . Unlike the majority of known cases, where practically ideal two-dimensional magnets are obtained by intercalation of previously grown single crystals, generally to the detriment of their crystal structure, the compounds under study permit one to do this correctly [*sic*].

The present paper is devoted to the study of the rf properties and magnetic phase transitions in one of the members of this family: $(\text{NH}_3)_2(\text{CH}_2)_3\text{MnCl}_4$ —propylene diammonium tetrachloromanganate, or PDAMnCl₄—over a wide range of frequencies and magnetic fields. As we show below, this compound exhibits a four-sublattice relativistically canted magnetic structure and displays the aforementioned features of the static and dynamic properties of low-dimensional systems.

II. STRUCTURE AND MAGNETIC PROPERTIES OF PDAMnCl₄

The crystal-chemical cell of PDAMnCl₄ is illustrated in Fig. 1. It contains four formula units ($z = 4$) and exhibits the layered structure of this antiferromagnet. The organic molecules $\text{NH}_3-(\text{CH}_2)_3-\text{NH}_3$ which separate the nearly square two-dimensional networks of manganese ions are situated vertically in the cell; for simplicity they are not shown here. According to the data of Ref. 8, the parameters of the crystal lattice are $a = 7.17 \text{ \AA}$, $b = 19.0 \text{ \AA}$, $c = 7.36 \text{ \AA}$, and the space group is *Imma*. The distance between nearest-neighbor Mn^{2+} ions is 5.2 \AA within a layer of 9.5 \AA for neighbors belonging to different layers. Studies⁹ of the magnetic properties of PDAMnCl₄ have determined that $T_N = 43 \text{ K}$, that the intralayer exchange interaction constant is $J = 4.6 \text{ K}$ (corresponding to an exchange field $2H_c = 1360 \text{ kOe}$), that the easy axis of anisotropy is **b** and that the spin-flop transition field is $H_{sf} = 24.2 \text{ kOe}$ and have detected the presence of a weak ferromagnetic moment along the *b* and *c*

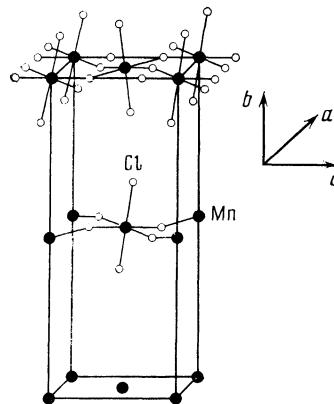


FIG. 1. Crystal-chemical cell of PDAMnCl₄.

axes. Jumping ahead, we note that the finding of a weak magnetic moment in the entire *bc* plane was puzzling to the authors of Ref. 9 and was evidently due to the poor quality of the samples.

After commencement of the present studies on the magnetic resonance in PDAMnCl₄, it became obvious that samples thicker than 0.3–0.5 mm contained crystallites in which the *c* and *a* axes were rotated by an angle close to 90° (this was clearly seen in the AFMR studies in a transverse field perpendicular to the easy axis). In addition, it is clear that in crystals with rhombic symmetry, if one ignores the possibility of screw structures or inhomogeneous states, the weak ferromagnetic moment should be oriented along one of the crystallographic axes.

More-serious contradictions arise if one attempts to explain in the framework of the previously⁸ established space group *Imma* the presence in PDAMnCl₄ of both weak ferromagnetism and a four-sublattice structure, which is indicated by the exchange modes which we detected in this antiferromagnet (a preliminary report of our observation of optical modes is given in Ref. 6). We therefore made an x-ray diffraction study of PDAMnCl₄ at room temperature. We used single crystals with a mass of 0.5–1 mg and monitored for the absence of twins by means of AFMR. Since the analogous salt with Cu^{2+} as the magnetic ion, PDACuCl₄, has space group *Pnma*, it was natural to conjecture the presence of *Pnma* in PDAMnCl₄.¹¹ Studies done on a Syntax diffractometer confirmed this conjecture. In a data block of 700 reflections we did not observe a single reflection whose extinction law was inconsistent with *Pnma*. Therefore, we shall assume in the following that the space group of PDAMnCl₄ is *Pnma*. In view of the absence of structural phase transitions between room temperature and T_N , we can extend this assumption to the low-temperature region as well.

III. EXPERIMENTAL TECHNIQUES

The studies of the resonance properties of PDAMnCl₄ were done using a pulsed millimeter-range spectrometer which permitted studying the angular and temperature dependences of the resonance field at liquid-helium temperatures.

The spectrometer was assembled in a reflected-wave scheme. The microwave power sources were either reflex klystrons (in the 1.5 cm–4 mm range) or backward wave tubes (in the 4–1.5 mm range), and a hybrid (magic) tee was used in the microwave bridge of the spectrometer. At wavelengths $\lambda \approx 4$ mm and shorter the power was transferred by oversize waveguides. Standard waveguides were used at wavelengths $\lambda \geq 8$ mm.

Unlike the pulsed spectrometers of the familiar designs, in which a shorted segment of the waveguide is used as the measurement cell, our spectrometer used a resonator, which gave a sharp increase in the sensitivity of the spectrometer and permitted observation of weak absorption lines with integrated intensities three orders of magnitude lower than that of the ordinary AFMR.

The sample was placed in a silver-plated German-silver resonator of the reflection type, with a loaded Q of ~ 1000 . The sample was mounted on a turntable which permitted changing the direction of the external field with respect to the axes of the crystal with an error of $\pm 1^\circ$ or less. The power absorbed by the sample was detected in an arrangement consisting of a detector, wide-band amplifier, and storage oscilloscope.

Magnetic fields up to 250 kOe were produced by discharging an IM5-140 capacitor bank (35 capacitors) through a solenoid impregnated with an epoxy compound. The magnetic-field pulse had a rise time of 10 msec. During its operation the solenoid was cooled to liquid-nitrogen temperature.

The frequency of the microwave oscillators was measured to an accuracy of 0.01% by VST frequency meters for the corresponding ranges. The field was calibrated by the ESR and AFMR signals of MnF_2 and diphenyl picryl hydrazyl (DPPH) crystals. The total uncertainty in the determination of H_{res} was 2%.

The PDAMnCl₄ crystals were grown by the slow evaporation at room temperature of a saturated solution of 1,3-propylene diamine hydrochloride and $MnCl_2 \cdot 4H_2O$ in water. Single-crystal samples with a mass of 1–5 mg were used in the experiments. In Figs. 3–6 below we show the antiferromagnetic resonance frequencies as a function of the magnetic field H for different orientations of H with respect to the crystallographic axes. Let us now turn to a discussion of the results.

VI. THEORY. COMPARISON WITH EXPERIMENT

1. Space group of the crystal. Hamiltonian of the system

As we have mentioned, the crystal-chemical unit cell of PDAMnCl₄ contains four magnetic atoms Mn^{2+} . For such an antiferromagnet the linear combinations of spin operators which realize the irreducible representations of the symmetry group of the paramagnetic phase are of the form

$$\begin{aligned} F &= s_1 + s_2 + s_3 + s_4 = F_1 + F_2, & C &= s_1 + s_2 - s_3 - s_4 = L_1 + L_2, \\ G &= s_1 - s_2 + s_3 - s_4 = F_1 - F_2, & A &= s_1 - s_2 - s_3 + s_4 = L_1 - L_2. \end{aligned} \quad (1)$$

Here, in accordance with the layered structure of the crystal, we have introduced the antiferromagnetism and ferromagnetism vectors

$$\begin{aligned} L_1 &= s_1 - s_3, & L_2 &= s_2 - s_4, \\ F_1 &= s_1 + s_3, & F_2 &= s_2 + s_4 \end{aligned} \quad (2)$$

for the first and second layers, respectively.

As we have mentioned, the existing data in the literature⁸ puts PDAMnCl₄ in the space group *Imma* (D_{2h}^{28}). However, in the framework of this space group one cannot explain the entire body of experimental data on the field dependence of the AFMR frequency. Table I gives the classification of the components of vectors (1) according to the irreducible representations of the group *Imma*. We note that the translation $t(1/2, 1/2, 1/2)$, representing atoms from different layers, is nontrivial, and the vectors (1) transform according to representations which are even with respect to inversion.

We see from Table I that depending on the sign of the interlayer exchange, the space group *Imma* admits the existence of either a two-sublattice antiferromagnet with weak ferromagnetism (the phase C_y, F_z or the phase F_y, C_z) or a four-sublattice antiferromagnet, but with a plane structure of the cross type (the phase A_y, G_z or the phase G_y, A_z). Therefore, we shall assume from here on that PDAMnCl₄ has the space group *Pnma* (D_{2h}^{16}) (see also Sec. II).

By acting on the components of the vectors (1) with the symmetry operations of space group *Pnma*, one can classify them according to the irreducible representations of this group (see Table II). Using Table II, one can easily write an invariant expansion of the Hamiltonian in the irreducible spin operators of the group.

TABLE I. Magnetic configurations irreducible with respect to space group *Imma* (D_{2h}^{28})

	E	C_{2x}	C_{2y}	C_{2z}	t	t_{2x}	t_{2y}	t_{2z}	
Γ_1	+	+	+	+	+	+	+	+	C_x
Γ_2	+	+	-	-	+	+	-	-	F_x
Γ_3	+	-	+	-	+	-	+	+	F_y
Γ_4	+	-	-	+	+	-	-	-	C_y
Γ_5	+	+	+	+	-	-	-	-	G_x
Γ_6	+	+	-	-	-	-	+	+	A_x
Γ_7	+	+	+	-	-	+	-	+	A_y
Γ_8	+	-	-	+	-	+	+	-	G_y
									C_z
									F_z
									G_z
									A_z

TABLE II. Magnetic configurations irreducible with respect to space group $Pnma (D_{2h}^{16})$

	E	C_{2x}	C_{2y}	C_{2z}	
Γ_1	+	+	+	+	C_x A_y G_z
Γ_2	+	+	-	-	F_x G_y A_z
Γ_3	+	-	+	-	G_x F_y C_z
Γ_4	+	-	-	+	A_x C_y F_z

For analysis of the role of the weak interlayer interaction in a quasi-two-dimensional magnet, it is convenient to represent the Hamiltonian of the system not in terms of the operators of the entire system (1) but in terms of the operators which refer to a single layer (2). Analysis of the experimental data and the results of subsequent calculations show that for describing the features of the AFMR and phase transitions in PDAMnCl₄ it is sufficient to choose a system Hamiltonian of the restricted form

$$\begin{aligned} \mathcal{H} = & -1/2 J_x (L_{1x}^2 + L_{2x}^2) - 1/2 J_y (L_{1y}^2 + L_{2y}^2) - 1/2 J_z (L_{1z}^2 + L_{2z}^2) \\ & + 1/2 I_x (F_{1x}^2 + F_{2x}^2) + 1/2 I_y (F_{1y}^2 + F_{2y}^2) + 1/2 I_z (F_{1z}^2 + F_{2z}^2) \\ & - D_{1x} (F_{1z} L_{1y} + F_{2z} L_{2y}) - D_{2x} (F_{1y} L_{1z} + F_{2y} L_{2z}) \\ & - \beta (L_{1x} L_{1y} - L_{2x} L_{2y}) - J_3 L_1 L_2 + I_3 F_1 F_2 - g \mu_B \mathbf{H} (F_1 + F_2). \end{aligned} \quad (3)$$

In this Hamiltonian the only interlayer interaction which is taken into account is the isotropic exchange. We have also neglected the Dzyaloshinskii interaction, which gives rise to a component F_{ix} in the layer. The validity of these assumptions will be justified by the results of our subsequent analysis.

The constants of the effective magnetic interactions in (3) are expressed linearly in terms of the intrasublattice and intersublattice exchange interaction constants and the anisotropy constant. Here the parameters J_α and I_α ($\alpha = x, y, z$) include the isotropic exchange interaction and part of the anisotropic interaction between spins within a layer; β is the intralayer anisotropy interaction of monoclinic symmetry; the parameters D_{1x} and D_{2x} are due to the Dzyaloshinskii interaction within a layer. Everywhere below we assume the following relationships among the parameters:

$$J_\alpha, I_\alpha \gg J_3, I_3, \quad D_{1x}, D_{2x} > |J_\alpha - J_{\alpha'}|, \beta, \quad (4)$$

which correspond to the experimental data.^{9,6} In Eq. (3) the g factor for the divalent ion Mn^{2+} in the state $^6s_{5/2}$ is assumed isotropic.

2. H||z. The Γ_4 phase (A_x, D_y, F_z)

a. The ground state of the system. In the low-dimensional magnet PDAMnCl₄ the symmetry class of the layers is lower than the symmetry class of the crystal as a whole. The weakness of the exchange interaction between layers substantially enhances the role of the relativistic interactions, and the magnetic structure of such a system turns out to be substantially noncollinear (a relativistically canted structure).

Earlier studies⁹ of the magnetic properties of PDAMnCl₄ have shown that in this compound: 1) the mag-

netic moments in the layers are ordered antiferromagnetically ($s_1 \uparrow s_3, s_2 \uparrow s_4$); 2) the easy axis of anisotropy is the y axis; 3) the system has a weak ferromagnetic moment $F \neq 0$. The first condition implies that the configuration of the magnetic moments in the ground state can be either the **C** or **A** type. The second condition implies that it is either C_y or A_y . The third condition, together with Table II, implies that the principal antiferromagnetism vector can only be C_y , since there is no magnetic moment in configuration A_y .

Thus, the magnetic configuration in the ground state of PDAMnCl₄ is A_x, C_y, F_z , which pertains to the representation Γ_4 . Its magnetic class $D_2(C_2)$ contains the transformations E, C'_{2x}, C'_{2y} , and C_{2z} ($'$ is the operation of time reversal). The configuration of the magnetic moments in the layers is illustrated in Fig. 2. Using (3), one can show that each layer is characterized by the following nonzero average values of the vectors:

$$\begin{aligned} L_{1y} = L_{2y} & \equiv 2sl_y, \quad L_{1x} = -L_{2x} \equiv 2sl_x, \\ F_{1z} = F_{2z} & \equiv 2sm_z, \quad m_z = H_D l_y / 2H_e, \end{aligned} \quad (5)$$

and the angle θ between the axis of easy magnetization y and the projection of the vector L_i onto the xy plane is determined from the relation

$$\tan 2\theta = H_{A3} (H_{A1} - H_{A2} + 2H_e' + H_{D1}^2 / 2H_e)^{-1}. \quad (6)$$

In formulas (5) and (6) we have used the following notation: $H_e \equiv s(J + I)\gamma^{-1}$ is the intralayer exchange field; $H_e' \equiv 2sJ_3\gamma^{-1}$ is the interlayer exchange field, $H_{A1} \equiv 2s(J_y - J_z)\gamma^{-1}$ is the uniaxial anisotropy field, which stabilizes the magnetic ordering along the y axis; $H_{A2} \equiv 2s(J_x - J_z)\gamma^{-1}$ is the rhombic anisotropy field:

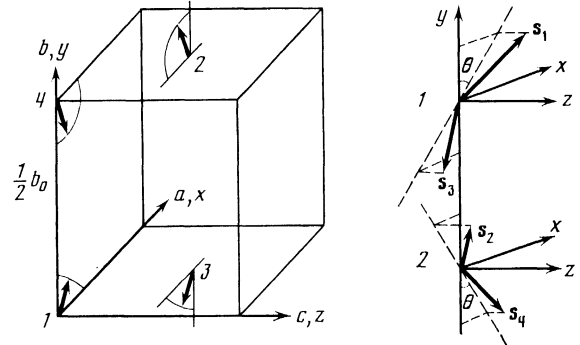


FIG. 2. Orientation of the spins of sublattices s_1, s_2, s_3 , and s_4 in the magnetic cell and their relative disposition in neighboring layers.

TABLE III. Classification of AFMR frequencies by symmetry types

Symmetry of magnetic ordering	Type of magnetic ordering	Symmetry of homogeneous vibrations	Number of resonance modes	Components of $\chi_{\alpha\beta}(\omega)$ having pole
$\Gamma_4(\mathbf{H}\ \mathbf{z})$	C_y	Γ_{14}	2 (AM + OM)	χ_{zz}
$\Gamma_3(\mathbf{H}\ \mathbf{y})$	C_z	Γ_{23}	2 (AM + OM)	$\chi_{xx}, \chi_{yy}, \chi_{xy}$
$\Gamma_{13}(\mathbf{H}\ \mathbf{y})$	C_z, C_x	Γ_{13}	2 (AM + OM)	χ_{yy}
		Γ_{24}	2 (AM + OM)	$\chi_{xx}, \chi_{zz}, \chi_{xz}$
		Γ_{13}	2 (AM + OM)	χ_{yy}
		Γ_{24}	2 (AM + OM)	$\chi_{xx}, \chi_{zz}, \chi_{xz}$

$H_{A3} \equiv 2s \cdot 2\beta\gamma^{-1}$ is the monoclinic anisotropy field; $H_{D1} \equiv 2s \cdot D_{1x} \gamma^{-1}$ is the Dzyaloshinskii field in a layer; $\gamma = g\mu_B$.

For our chosen magnetic structure of PDAMnCl₄, with principal antiferromagnetism vector C_y , we have $l_y > l_x$ even though, as we see from (6), the angle θ is not small for $H'_e \sim H_A$, i.e., the component l_x is of the same order of magnitude as l_y , and the magnetic configuration of the system is substantially noncollinear (see Fig. 2).

The imposition of an external magnetic field directed along the z axis does not alter the symmetry of the ground state of the system. The equilibrium state is determined, as before, by components (5), but now the ferromagnetic moment is due to the Dzyaloshinskii interaction and the field

$$m_z = (H + H_{D1}l_y) / 2H_e, \quad (7)$$

while the relationship between l_x and l_y is determined by the equation

$$(H_{A1} - H_{A2} + 2H'_e + H_{D1}^2 / 2H_e) l_x l_y + H_{D1} H l_x / 2H_e + 1/2 H_{A3} (l_y^2 - l_x^2) = 0. \quad (8)$$

We note that in accordance with general symmetry considerations,¹⁰ the Γ_4 phase will be stable at arbitrarily large fields, i.e., for $\mathbf{H}\|\mathbf{z}$ there is no spin-flip transition in the system.

b. Frequencies of homogeneous vibrations. The AFMR frequencies were calculated by the method proposed in Ref. 11. In this approach the equations of motion are written for irreducible (with respect to the group of the paramagnetic phase) linear combinations of spin operators (1). The classification of the frequencies of the homogeneous magnetic resonance by symmetry types is easily done using Table II with allowance for the role of unitary operations in this classification.^{11,12} The corresponding results for different directions of the external field are given in Table III. The Γ_4 phase corresponds to the first row of this table.

The oscillatory parts of the magnetic moments of the sublattices transform in this phase according to the two mixed representations Γ_{14} and Γ_{23} (see the third column of Table III). The frequencies of vibrations with symmetry Γ_{14} are given by

$$\gamma^{-2} \omega_{14A}^2 = 2H_e [(H_{A1} - H_{A2}) (l_y^2 - l_x^2) + 2H_{A3} l_x l_y] + H_{D1}^2 (l_y^2 - l_x^2) + H_{D1} H l_y, \quad (9)$$

$$\gamma^{-2} \omega_{14O}^2 = \gamma^{-2} \omega_{14A}^2 + 4H_e H'_e (l_y^2 - l_x^2).$$

Two frequencies with symmetry Γ_{23} are described by the expressions

$$\begin{aligned} \gamma^{-2} \omega_{23A}^2 &= 2H_e [H_{A1} l_y^2 + (H_{A2} - 2H'_e) l_x^2 + H_{A3} l_x l_y] \\ &\quad + (H + H_{D1} l_y) [H + 2(H_{D1} + H_{D2}) l_y] - H_{D2}^2 l_x^2, \\ \gamma^{-2} \omega_{23O}^2 &= \gamma^{-2} \omega_{23A}^2 + 4H_e H'_e (l_y^2 + l_x^2). \end{aligned} \quad (10)$$

Here, besides the parameters already introduced, we have used the notation: $H_{D2} \equiv 2s D_{2x} \gamma^{-1}$ is the Dzyaloshinskii field in a layer. Results (9) and (10) are given to an accuracy up to terms of order H_D^2 and $H_e H_A$.

For $H'_e \sim H_e$ formulas (9) and (10) go over to the familiar expressions for the frequencies of a four-sublattice antiferromagnet with weak ferromagnetism.^{2,11} Here, as we see from (6) or (8), $l_x \ll l_y$, i.e., the magnetic structure of the system is slightly canted. Further, Eqs. (9) and (10) imply that $\omega_{14A}, \omega_{23A} \ll \omega_{14O}, \omega_{23O}$ and sensibly divide the vibrations into acoustic and exchange modes. The frequencies of the first go as $\sim (H_e H_A)^{1/2}$, the frequencies of the second go as $\sim (H_e H'_e)^{1/2} \sim H_e$.

For $H'_e \sim H_A$, as we have mentioned, one has $l_x \sim l_y$, and the frequencies of the acoustic and optical modes become equal in order of magnitude, and neither of the pairs of frequencies can be obtained in the two-sublattice model. Thus, in the case of low-dimensional antiferromagnetic systems it is in principle impossible to describe the antiferromagnet in the two-sublattice model and to formally divide the frequencies into acoustic and optical modes.

The field dependence of the frequencies ω_{14A} and ω_{14O} are determined by the parameter H_{D1} , which is easily found from the slope of the experimental AFMR curves, while the field dependence of the frequencies ω_{23A} and ω_{23O} permit determination of the parameter H_{D2} . It also follows from (9) and (10) that the differences of the squares of the frequencies are

$$\omega_{14O}^2 - \omega_{14A}^2 = \gamma^2 \cdot 4H_e H'_e (l_y^2 - l_x^2), \quad (11)$$

$$\omega_{23O}^2 - \omega_{23A}^2 = \gamma^2 \cdot 4H_e H'_e (l_y^2 + l_x^2) \quad (12)$$

and are independent of the field in this approximation. The left-hand side of expressions (11) and (12) are determined experimentally. The ratio of the quantities in (11) and (12) determines the angle of inclination of the antiferromagnetism vector of the layer from the easy axis.

Knowing H_{D1}, H_{D2}, l_x, l_y , and H_e (the latter is deter-

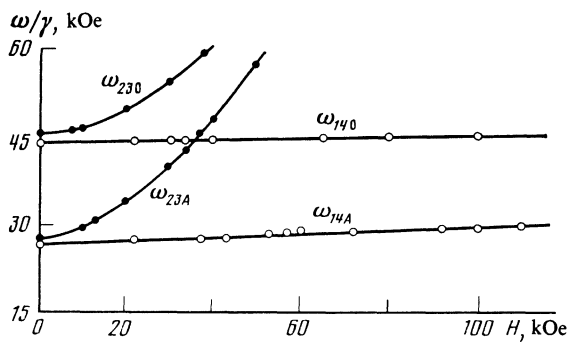


FIG. 3. Frequency-field diagram of the AFMR for $\mathbf{H}||\mathbf{z}$. The solid lines are the theoretical curves (9), (10); the points are experimental data. Here and in Figs. 4–6: ● $\mathbf{H}||\mathbf{h}$, ○ $\mathbf{H}||\mathbf{h}$, $T = 4.2$ K.

mined from independent measurements of the susceptibility⁹), one can use formulas (9) and (10) to find the remaining parameters of the system: H_{A1} , H_{A2} , H_{A3} , and H_e' . The values (in kOe) found in this way for the effective parameters of the magnetic susceptibility in $(\text{NH}_3)_2(\text{CH}_2)_3\text{MnCl}_4$ and the AFMR frequencies at $H = 0$ are:

$$\begin{aligned} H_{A1} &= 0.54, & H_{A2} &= 0.09, & H_{A3} &= 0.34, \\ 2H_e' &= 0.92, & H_{D1} &= 1.7, & H_{D2} &= 1.3, \\ & & 2\theta &= 14^\circ, \\ \gamma^{-1}\omega_{14A} &= 26.6, & \gamma^{-1}\omega_{23A} &= 27.7, \\ \gamma^{-1}\omega_{140} &= 43.9, & \gamma^{-1}\omega_{230} &= 44.9. \end{aligned}$$

Thus the presence of experimental data on all four frequencies permits a unique reconstruction of the magnetic structure of the compound under study and a determination of the values of all the effective magnetic interactions solely from the AFMR spectrum. The solid lines in Fig. 3 show the theoretical curves for the field dependence of the AFMR frequencies as calculated by formulas (9) and (10) with the above values of the effective fields.

c. The rf magnetic susceptibility tensor. According to the symmetry classification of the frequencies of the homogeneous resonance, the symmetry of the rf magnetic susceptibility tensor is determined by the magnetic symmetry class of the crystal and not by the symmetry class of the individual layers. The last column in Table III indicates which of the components of the rf magnetic susceptibility tensor $\chi_{\alpha\beta}(\omega)$ have a pole corresponding to vibrations of the given symmetry. As we know, a homogeneous rf field excites those resonance modes whose vibrations are accompanied by oscillation of the magnetic moment of the system. Table III gives the classification of the resonance modes and indicates which components of the rf susceptibility tensor have poles corresponding to these modes.

The components of the rf magnetic susceptibility tensor in the Γ_4 phase ($\mathbf{H}||\mathbf{z}$) are determined by the following expressions:

$$\chi_{zz}(\omega) = \chi_0 \left[\frac{\omega_{14A}^2}{\omega_{14A}^2 - \omega^2} + \frac{\gamma^2 (H_{D1} l_x)^2}{\omega_{140}^2 - \omega^2} \right], \quad (13a)$$

$$\chi_{xx}(\omega) = \chi_0 \left\{ \frac{\omega_{23A}^2 + \gamma^2 K_1}{\omega_{23A}^2 - \omega^2} + \frac{\gamma^2 [H + (H_{D1} + H_{D2}) l_y]^2 l_x^2}{\omega_{230}^2 - \omega^2} \right\}, \quad (13b)$$

$$\chi_{yy}(\omega) = \chi_0 \gamma^2 \left\{ \frac{[(H + H_{D1} l_y) l_y - H_{D2} l_x^2]^2}{\omega_{23A}^2 - \omega^2} + \frac{K_2}{\omega_{230}^2 - \omega^2} \right\}, \quad (13c)$$

$$\begin{aligned} \chi_{xy}(\omega) &= -\chi_{yx}(\omega) = i\omega\gamma (H + H_{D1} l_y) \\ &\times \left\{ (\omega_{23A}^2 - \omega^2)^{-1} \right. \\ &\left. - \frac{H + (H_{D1} + H_{D2}) l_y}{H + H_{D1} l_y} \frac{\gamma^2 \cdot 4H_e H_e' l_x^2}{(\omega_{23A}^2 - \omega^2)(\omega_{230}^2 - \omega^2)} \right\}, \quad (13d) \end{aligned}$$

where

$$\begin{aligned} K_1 &= (H_{D2} l_x)^2 - [H + (H_{D1} + H_{D2}) l_y]^2 l_x^2 - 2H_e [(H_{A2} - 2H_e') l_x^2 \\ &\quad + \frac{1}{2} H_{A3} l_x l_y], \quad (14) \end{aligned}$$

$$\begin{aligned} K_2 &= 2H_e [H_{A2} l_x^2 + \frac{1}{2} H_{A3} l_x l_y] + (H + H_{D1} l_y)^2 \\ &\quad - [(H + H_{D1} l_y) l_y - H_{D2} l_x^2]^2, \quad (15) \end{aligned}$$

$\chi_0 \equiv 2s\gamma/H_e v_0$; v_0 is the volume of the magnetic cell.

Let us briefly discuss these expressions. The optical mode corresponding to the symmetric vibration with frequency ω_{140} is excited only for $\mathbf{h}||\mathbf{z}$. We see that the intensity of the absorption is practically independent of the field and is determined by two factors: 1) the degree to which the magnetic structure is canted—the ratio l_x/l_y ; 2) the value of the Dzyaloshinskii interaction within a layer. The asymmetric optical mode with frequency ω_{230} is excited for $\mathbf{h}||\mathbf{z}$ and has a substantially higher intensity than the symmetric optical mode. In this case the highest absorption intensity in weak fields $H \ll (H_e H_A)^{1/2}$ is for $\mathbf{h}||\mathbf{y}$, and for $H \gtrsim (H_e H_A)^{1/2}$ the intensity of the absorption is practically independent of the direction of \mathbf{h} in the xy plane and is proportional to H^2 . This picture corresponds completely to the experimental results.

The specific features of low-dimensional magnets are also manifested in the static susceptibility. To obtain the static susceptibility one must set $\omega = 0$ and expand (13) in a series in the field after making the replacements

$$H \rightarrow H_z, \quad h_x \rightarrow H_x, \quad h_y \rightarrow H_y, \quad h_z \rightarrow H_z.$$

As a result we obtain²⁾

$$\begin{aligned} \chi_{zz}(0) &= \chi_0 [1 + (H_{D1} l_x)^2 \gamma^2 / \omega_{140}^2], \\ \chi_{xx}(0) &= \chi_0 [1 + \gamma^2 K_1 / \omega_{23A}^2 + \gamma^2 (H_{D1} + H_{D2})^2 l_x^2 l_y^2 / \omega_{230}^2], \quad (16) \\ \chi_{yy}(0) &= \chi_0 [(H_{D1} l_y^2 - H_{D2} l_x^2) \gamma^2 / \omega_{23A}^2 + \gamma^2 K_2 / \omega_{230}^2], \end{aligned}$$

where ω_{140} , ω_{23A} , K_1 , and K_2 are determined by formulas (9), (10), (14), and (15) for $H = 0$.

Expressions (16) demonstrate the two characteristic features of the systems under study. First, we see that the static longitudinal susceptibility $\chi_{yy}(0)$ becomes comparable in magnitude to the transverse susceptibility $\chi_{xx}(0)$ or $\chi_{zz}(0)$. This is a direct consequence of the substantial canting of the system. Another manifestation of the canting is the difference of the transverse components of the static susceptibility tensor from the usual value $\chi_0 = 2s\gamma/H_e v_0$. This is

due to the appearance of the so-called twisting susceptibility in a four sublattice canted antiferromagnet.

In the case of $\chi_{zz}(0)$ an external field imposed along the magnetic moment of a monoclinic layer causes not only a bending of the magnetic moments of the sublattices toward the direction of the field but also a rotation of these moments about an axis along the field direction [as is seen from an analysis of expression (8), the canting angle θ decreases with increasing field]. For such a field direction the symmetry of the initial phase is not broken. In the three-dimensional case $H_e \sim H_e$, this effect is very small, of order $H_D^2 H_A^2 / H_e^4$. In the low-dimensional case the antiferromagnetism vectors of the layers are weakly intercoupled and the twisting effect is enhanced, having an order of magnitude $H_D^2 / H_e H_e'$.

3.H||y. Phase transitions

An external magnetic field directed along the y axis gives rise to a nonzero magnetic moment along this axis and thus to nonzero antiferromagnetism vectors G_x and C_z (see Table II). As a result, the system exhibits a mixed magnetic configuration described by the irreducible representation Γ_{34} [magnetic class $C_2(C_1)$, with elements E and C'_{2x}]. As we know, an external field which breaks the magnetic symmetry of a system induces magnetic phase transitions in it. The classification of magnetic phase transitions in low-dimensional magnets is no different from the corresponding classification in three-dimensional systems. However, as we shall see below, the physical picture of the transition can be substantially different.

The experimental curves for the AFMR frequency versus the field in PDAMnCl₄ (Fig. 4) show that this low-dimensional four-sublattice antiferromagnet exhibits a first-order phase transition at $H = 24.6$ kOe as the field is increased along the easy axis. We see from Table II that, depending on the relationship of the anisotropy constants, a

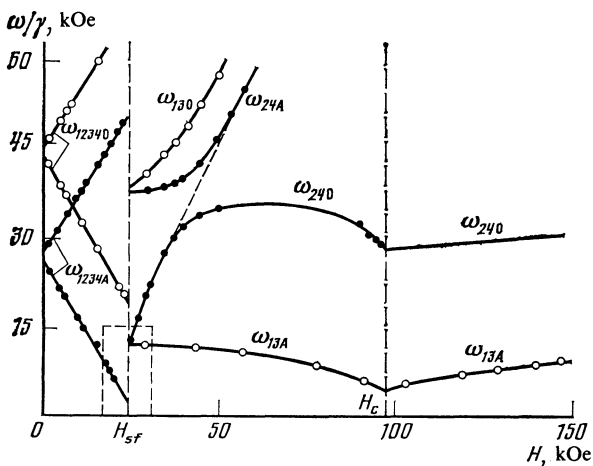


FIG. 4. Frequency-field diagram of the AFMR for $H||y$. The region enclosed in the dashed lines is shown in Fig. 5. The solid lines at fields $H < H_c$ are drawn through the experimental points, while for $H > H_c$ they were given by the formulas $\gamma^{-2}\omega_{\text{exp}}^2 = \Delta^2 + \gamma^{-2}\omega^2(H)$, where $\omega^2(H)$ are the theoretical curves (34).

field along the easy axis can induce a transition either to the Γ_3 phase [magnetic class $D_2(C_2)$, with symmetry elements E , C'_{2x} , C_{2y} , and C'_{2z}] or to the Γ_{13} phase [magnetic class $C_2(C_2)$, with elements E and C_y] or to the Γ_{23} phase [magnetic class $C_2(C_1)$, with elements E and C'_{2z}].

We see from Table II that the transition to the Γ_{23} phase involves the destruction of the principal antiferromagnetism vector. At such a phase transition there should be a softening of an optical mode. In PDAMnCl₄ the experiments reveal the softening of an acoustic mode, so that the phase transition in the system at $H = 24.6$ kOe must be either to the Γ_3 or Γ_{13} phase.

Experiments reveal yet another mode softening at a field $H = 98$ kOe, indicating the presence of a second-order magnetic phase transition. We note that the y axis is an odd axis for the vector C (the vector C changes sign under the operation C_{2y}). Since the magnetic structure is even with respect to inversion, there is no spin-flip transition in the system at arbitrarily large fields parallel to the odd axis.¹⁰ We also note that the spin-flip transition in this compound should occur at much higher fields $H \sim H_e$. At the same time, a second-order spin-orientation phase transition can occur if the system enters the Γ_{13} phase as a result of the spin-flop transition. Then the following sequence of phase transitions is possible. When H reaches the value H_{sf} there is a discontinuous reorientation of the principal antiferromagnetism vector from the y axis to a direction close to the x axis. Then, in the field interval $H_{sf} < H < H_c$, the presence of an interaction of the form $D_{2x}(L_{1z}F_{1y} + L_{2z}F_{2y})$ will cause the principal antiferromagnetism vector to rotate from the direction close to the x axis toward alignment with the z axis. At $H > H_c$ the system undergoes a transition to the Γ_3 phase.

a. Spin-flop transition. To study the spin-flop transition in the given system we shall start from Hamiltonian (3), which neglects the Dzyaloshinskii interaction within the layers. Such an approximation corresponds to a four-sublattice antiferromagnet with a structure of the plane cross type.

In the equilibrium state this plane cross model gives

$$l_{1x} = -l_{2x} \equiv l_x, \quad l_{1y} = -l_{2y} \equiv l_y, \quad m_{1x} = -m_{2x} \equiv m_x, \quad m_{1y} = m_{2y} \equiv m_y \quad (17)$$

for the Γ_{34} phase and

$$l_{1x} = l_{2x} \equiv l_x, \quad l_{1y} = -l_{2y} \equiv l_y, \quad m_{1x} = -m_{2x} \equiv m_x, \quad m_{1y} = m_{2y} \equiv m_y \quad (18)$$

for the Γ_{13} phase. Here we are neglecting the projections of the vectors l and m onto the z axis: for m because m_z is due solely to the Dzyaloshinskii interaction and is small; for l because l_z exists only in the Γ_3 phase, and we are assuming that the admixture of this phase is still small. These relationships allow us to reduce the calculation of the equilibrium potential of the rhombic system to a calculation of the equilibrium potential of a monoclinic layer. For example, in the Γ_{34} phase we have

$$(2s)^{-2}\Phi_{34} = -J_x l_x^2 - J_y l_y^2 + I_x m_x^2 + I_y m_y^2 + I_s (m_y^2 - m_x^2) - 2\beta l_x l_y - 2\gamma H m_y (2s)^{-1}. \quad (19)$$

We introduce the angle θ giving the deviation of the antiferromagnetic moment of the layer from the easy axis. Then

$$l_x = -l \sin \theta, \quad l_y = l \cos \theta, \quad m_x = m \cos \theta, \quad m_y = m \sin \theta. \quad (20)$$

Relation (20) already incorporates the orthogonality conditions $\mathbf{m} \cdot \mathbf{l} = 0$; substituting them into the potential and taking into account that $l^2 = 1 - m^2$, we have with accuracy to terms of order $H_A m^2$

$$(2s\gamma)^{-1} \Phi_{34} = -(H_e + H_e') + 2H_e' \sin^2 \theta + 2H_e m^2 - 2Hm \sin \theta + (H_{A1} - H_{A2}) \sin^2 \theta - H_{A3} \sin \theta \cos \theta, \quad (21)$$

where for convenience in the calculations which follow we have converted to the effective interaction fields introduced earlier.

Potential (21) is still inconvenient for analysis, since the magnitude of the magnetic moment \mathbf{m} of a layer is a function of the angle θ . However, in this case, when the relativistic interactions are much weaker than the exchange interaction, the dependence of \mathbf{m} on \mathbf{H} can be found by the method of successive approximations. In the leading approximation we find from the minimum of (21)

$$m = H \sin \theta / 2H_e. \quad (22)$$

Substituting (22) into (21), we obtain for the thermodynamic potential

$$(2s\gamma)^{-1} \Phi_{34} = -(H_e + H_e') + (H_{A1} - H_{A2} + 2H_e' - H^2/2H_e) \sin^2 \theta - \frac{1}{2} H_{A3} \sin 2\theta. \quad (23)$$

The subsequent analysis of expression (23) is done in the standard way.

The equilibrium value of the angle θ in the Γ_{34} phase is described by the expression

$$\operatorname{tg} 2\theta = H_{A3} (H_{A1} - H_{A2} + 2H_e' - H^2/2H_e)^{-1}. \quad (24)$$

By making the replacement $H_e' \rightarrow -H_e'$ in (23) and (24), we obtain the relations describing the behavior of the system in the Γ_{13} phase. The thermodynamic potential of the phases become equal in a field

$$H_{sf}^2 = 2H_e (H_{A1} - H_{A2}). \quad (25)$$

Curiously, expression (25) does not depend on H_e' and coincides with the value H_{sf} for a two-sublattice rhombic antiferromagnet.

To determine the stability boundaries of the phases we must actually repeat the same calculations but now for the nonequilibrium potential, with each layer being described by its own vectors \mathbf{l} and \mathbf{m} in (19). It can be shown that the Γ_{34} phase is stable in fields $H < H_{34}$, where

$$H_{34}^2 = H_{sf}^2 + 2H_e H_e' - 2H_e [(H_e' + H_{A3})(H_e' - H_{A3})]^{1/2}, \quad (26)$$

and the Γ_{13} phase is stable starting at fields $H > H_{13}$:

$$H_{13}^2 = H_{sf}^2 - 2H_e H_e' + 2H_e [(H_e' + H_{A3})(H_e' - H_{A3})]^{1/2}. \quad (27)$$

Formulas (26) and (27) are valid for $H_e' \gg H_{A3}$. For $H_e' < H_{A3}$ the Γ_{34} and Γ_{13} phases are stable in all fields.

From these results we can infer the following physical

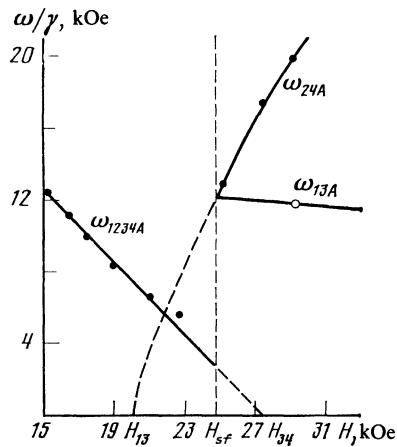


FIG. 5. Frequency-field diagram of the AFMR in the vicinity of the spin-flop transition. The dashed lines give the extrapolation of the experimental $\omega(H)$ curves to $\omega = 0$.

picture of the spin-flop transition. As the field along the easy axis increases, there is an increase in the angle between the antiferromagnetism vectors of the layer. This occurs at a cost of interlayer exchange energy. However, if $H_e' > H_A$, then one of the antiferromagnetism vectors of the layer can overcome the potential barrier due to the anisotropic interaction. Then, by abruptly changing its direction by almost 180° , it wipes out the cost in exchange energy—the principal antiferromagnetism vector rotates 90° and a spin-flop transition occurs in the system. Clearly, if H_e' is not much greater than the anisotropy parameter, the stability region of the phases can be rather wide, but finite.

If, on the other hand, the energy of the interlayer exchange is insufficient to overcome the potential barrier of the anisotropic interaction, $H_e' < H_{A3}$, then the two phases are stable over the entire field interval $H < H_e$.

In PDAMnCl₄ we have $H_e' > H_{A3}$, and a spin-flop transition is observed, with indications that the antiferromagnetic and spin-flop phases are stable over a wide region of fields beyond the point H_{sf} (Fig. 5). Substituting into (26) and (27) the numerical values of the parameters obtained in part 2b of Sec. IV, we find that $H_{34} = 28.2$ kOe and $H_{13} = 20$ kOe. These values are in good agreement with the values obtained by extrapolating the experimental $\omega(H)$ curve to $\omega = 0$ (Fig. 5).

Near the spin-flop transition field, finite antiferromagnetic samples exhibit a so-called intermediate state.¹³ This state has its origins in the presence of demagnetization in magnets of finite dimensions, and the field interval in which it exists is proportional to the jump Δm in the magnetization between the spin-flop and antiferromagnetic phases. A simple calculation using formulas (22) and (24) and the parameters of the effective fields from part 2b of Sec. IV shows that $\Delta m \sim 10^{-3}$ in PDAMnCl₄, i.e., the existence region of the intermediate state is extremely narrow.

b. Spin-reorientation transition. In the Γ_{13} phase the equilibrium values of the antiferromagnetism vectors and magnetic moment of the layers satisfy the condition (see

Table II)

$$l_{1x}=l_{2x}\equiv l_x, \quad l_{1y}=-l_{2y}\equiv l_y, \quad l_{1z}=l_{2z}\equiv l_z, \\ m_{1x}=-m_{2x}\equiv m_x, \quad m_{1y}=m_{2y}\equiv m_y, \quad m_{1z}=-m_{2z}\equiv m_z.$$

Using these conditions, the thermodynamic potential of a four-sublattice rhombic antiferromagnet can be reduced to the potential of a two-sublattice antiferromagnet; the latter, to terms of order $H_A m^2$, is of the form

$$(2s\gamma)^{-1}\Phi_{13} = -(H_e + H_e') - H_{A2}l_x^2 + (2H_e' - A_{A1})l_y \\ + H_e m^2 - 2H_{D1}l_y m_z - 2H_{D2}l_z m_y - H_{A3}l_x l_y - 2H m_y. \quad (28)$$

Potential (28) corresponds to the potential of a two-sublattice antiferromagnet of monoclinic symmetry, where the only operation C_{2z} is odd. In this case a field along the y axis induces only a single phase transition of the spin-reorientation type.

As in the analysis of the spin-flop transition, we use condition (4) to eliminate the vector \mathbf{m} from the thermodynamic potential. We note that at the given spin-reorientation transition the magnetic moments of the sublattices execute a rather complicated motion in space. Therefore, we write the expression for \mathbf{m} which satisfies the minimum of the thermodynamic potential in vector form¹⁴:

$$\mathbf{m} = [1 \times [\tilde{\mathbf{H}} \times 1]] / 2H_e. \quad (29)$$

The field $\tilde{\mathbf{H}}$ appearing in expression (29) is the effective field which gives rise to \mathbf{m} . In our case ($\mathbf{H} \parallel y$)

$$\tilde{H}_x = 0, \quad \tilde{H}_y = H + H_{D2}l_z, \quad \tilde{H}_z = H_{D1}l_y.$$

We introduce for the vector \mathbf{l} a spherical coordinate system with polar axis z and azimuthal axis x . Then a polar angle $\theta = 0$ will correspond to the Γ_3 phase, and the order parameter of the given second-order transition will thus be the angle θ .

Using (29), we can easily find the values of the components of the vector \mathbf{m} . Substituting them into the thermodynamic potential and minimizing with respect to the angle φ , we have near the phase transition point

$$(2s\gamma)^{-1}\Phi_{13} = \text{const} + \Lambda(H, \varphi_0)\theta^2 + \dots, \quad (30)$$

$$\Lambda(H, \varphi_0) = -H_{A2} + \frac{H_{D2}}{2H_e}(H + H_{D2}) + \left[H_{A2} - H_{A1} + 2H_e' \right. \\ \left. + \frac{H + H_{D2}}{2H_e}(H + H_{D2} + 2H_{D1}) \right] \sin^2 \varphi_0 - \frac{1}{2} H_{A3} \sin 2\varphi_0,$$

and the equilibrium value of the angle $\varphi = \varphi_0$ is determined by the expression

$$\tan 2\varphi_0 = H_{A3} \left\{ 2H_e' + H_{A2} - H_{A1} \right. \\ \left. + \frac{H + H_{D2}}{2H_e}(H + H_{D2} + 2H_{D1}) \right\}^{-1}. \quad (31)$$

The value of the phase transition field H_c is found from the condition $\Lambda(H_c, \varphi_0) = 0$. Substituting (31) into this condition we have

$$[2H_e H_{A2} - H_{D2}(H_c + H_{D2})] \{2H_e(2H_e' - H_{A1}) \\ + (H_c + H_{D2})[H_c + 2(H_{D1} + H_{D2})]\} + H_e^2 H_{A3}^2 = 0. \quad (32)$$

Using the values of the effective magnetic interactions in PDAMnCl₄ (see part 2b of Sec. IV), we obtain for this crystal the value $H_c = 98$ kOe, in good agreement with experiment. The agreement, however, must to a certain degree be regarded as accidental. In fact, as we see from (32), a change in the value of H_{A2} , for example, by only 10 Oe (10% of H_{A2}) leads to a change in H_c by ~ 10 kOe.

4. $\mathbf{H} \parallel y$. The rf properties

The Γ_3 phase

a) AFMR frequencies. The ground state in the Γ_3 phase ($H > H_c$) is the magnetic configuration G_x, F_y, C_z which is invariant under the symmetry operations E, C'_{2x}, C_{2y} , and C'_{2z} of the magnetic class $D_2(C_2)$. In the general case this configuration corresponds to a four-sublattice antiferromagnet. However, we can easily satisfy ourselves that for the actual relationship of the parameters in PDAMnCl₄ [see the expression for Hamiltonian (3)] the magnetization vector in the layer has no projection onto the x axis: $F_{1x} = F_{2x} = 0$. Thus $G_x = 0$, and the static configuration of the magnetic moments of the system actually assumes a two-sublattice nature. It is characterized by the components l_z and m_z of the antiferromagnetism and magnetization vectors of the layer:

$$m_y = (H + H_{D2}l_z) / 2H_e. \quad (33)$$

Although statically the system has a two-sublattice nature, its dynamic properties are fundamentally different from those of a two-sublattice antiferromagnet; the effects of the many-sublattice nature are a factor of $H_e/H_e' \gg 1$ stronger in low-dimensional systems than in three-dimensional systems.

Let us find the AFMR frequencies in this phase. As Table II implies, the oscillatory parts of the magnetic moments of the sublattices transform according to the two representations Γ_{13} and Γ_{24} . The corresponding calculation of the AFMR frequencies gives

$$2\gamma^{-2}\omega_{13A,0}^2 = 2H_e(2H_e' - H_{A1} - H_{A2})l_z^2 \\ + (H + H_{D2}l_z)[H + (2H_{D1} + 3H_{D2})l_z] \\ \pm (2H_e(2H_e' + H_{A2} - H_{A1})l_z^2 \\ + (H + H_{D2}l_z)[H + (H_{D2} + 2H_{D1})l_z])^2 \\ + 4H_e^2 H_{A3}^2 l_z^4)^{1/2}, \quad (34a)$$

$$2\gamma^{-2}\omega_{24A,0}^2 = 2H_e(2H_e' - H_{A1} - H_{A2})l_z^2 \\ + (H + H_{D2}l_z)[H + (2H_{D1} + 3H_{D2})l_z] \\ \pm (2H_e(-2H_e' + H_{A2} - H_{A1})l_z^2 \\ + (H + H_{D2}l_z)[H + (H_{D2} + 2H_{D1})l_z^2])^2 \\ + 4H_e^2 H_{A3}^2 l_z^4)^{1/2}. \quad (34b)$$

We note first of all that for $H_{A3} = 0$ the AFMR frequencies in the Γ_3 phase [Eq. (34)] go over to the frequencies in the Γ_4 phase (Eqs. (9) and (10)) and vice versa with the following relabeling of the variables:

$$\omega_{13A}(\Gamma_3) \leftrightarrow \omega_{14A}(\Gamma_4), \quad \omega_{24A}(\Gamma_3) \leftrightarrow \omega_{23A}(\Gamma_4), \\ \omega_{13O}(\Gamma_3) \leftrightarrow \omega_{23O}(\Gamma_4), \quad \omega_{24O}(\Gamma_3) \leftrightarrow \omega_{14O}(\Gamma_4).$$

This property becomes obvious when we recognize that for $H_{A3} = 0$ we have $l_x = 0$ in the Γ_4 phase and, as follows from Table II, the phases Γ_3 and Γ_4 differ only in the choice of coordinate axes.

For $H'_e \sim H_e$ we can neglect terms of order H_{A3}^2/H_e^2 . Further, it follows from (34) that $\omega_{13O}, \omega_{24O} \gg \omega_{13A}, \omega_{24A}$ and it is meaningful to divide the vibrations into acoustic and optical modes. Here the expressions for the acoustic modes coincide with the expressions for the AFMR frequencies of a two-sublattice antiferromagnet.

When $H'_e \sim H_A$, all the frequencies are of the same order, and the formal division of the frequencies into acoustic and exchange modes vanishes. Thus, even in the case of collinear structures there is no region of frequencies in which a low-dimensional four-sublattice system can be reduced to an effective two-sublattice system.

We note that it is only for $H'_e = 0$ that the frequencies (34) coincide in pairs so that even dynamically the system acquires a two-sublattice nature. In the Γ_3 phase, unlike the Γ_4 phase, frequencies of different symmetry coincide in pairs for $H'_e = 0$.

The frequency ω_{13A} (34a) goes to zero at $H = H_c$ (32). At the same time, experiment shows (see Fig. 4) that $\gamma^{-1}\omega_{13A}^{\text{exp}} = \Delta = 4.6$ kOe at the phase transition point. The experimental curve of $\gamma^{-1}\omega_{13A}^{\text{exp}}$ is well described by the expression

$$[\gamma^{-1}\omega_{13A}^{\text{exp}}(H)]^2 = \Delta^2 + \omega_{13A}^2(H)\gamma^{-2},$$

where $\omega_{13A}(H)$ is determined by formula (34a). The nature of the gap Δ in the soft mode spectrum is unquestionably an interesting problem.

We note that the thermodynamic potential of the system, with allowance for the interaction with the lattice in the Γ_{13} phase, contains an invariant of the form

$$(bC_x + b'A_y)C_z u_{xz},$$

or, in terms of the order parameter

$$(b \sin \varphi + b' \cos \varphi) \theta u_{xz}. \quad (35)$$

Here b and b' are linear combinations of the components of the magnetoelastic-constant tensor (they have dimensions of effective magnetic fields), and u_{xz} is a component of the strain tensor. It follows from (35) that the given spin-reorientation transition is a proper ferroelastic transition. As is shown in Refs. 15 and 16, in this case the soft mode spectrum exhibits a gap of magnetoelastic origin. Omitting the awkward calculations, we get for the striction gap at the phase transition point

$$\gamma^{-2}\Delta\omega_{13A,3}^2 = 2H_c(b \sin \varphi_0 + b' \cos \varphi_0)^2 (4C_{xxxx})^{-1}, \quad (36)$$

where C_{xxxx} is a component of the elastic-constant tensor, and the equilibrium angle φ_0 in the given approximation is determined by expression (31) with H equal to the value of H_c found from (32) without allowance for the magnetostriction. However, we do not know the values of the elastic and magnetoelastic constants of the crystal, and the question of whether expression (36) agrees with experiment will require additional studies.

b. The rf magnetic susceptibility tensor. The last column in Table III indicates which components of the rf magnetic susceptibility tensor have poles corresponding to the vibrations of the given symmetry. It follows from the table that in the Γ_3 phase the component $\chi_{yy}(\omega)$ has poles corresponding to vibrations of symmetry Γ_{13} , and the components $\chi_{xx}(\omega)$, $\chi_{zz}(\omega)$, $\chi_{xz}(\omega)$, and $\chi_{zx}(\omega)$ have poles corresponding to vibrations of symmetry Γ_{24} . Thus the AFMR frequencies $\omega_{13A,0}$ are excited by an rf field $\mathbf{h} \parallel \mathbf{y}$ and the frequencies $\omega_{24A,0}$ by an rf field $\mathbf{h} \parallel \mathbf{y}$.

Let us give explicit expressions for the components of the rf magnetic susceptibility tensor in the Γ_3 phase:

$$\begin{aligned} \chi_{yy}(\omega) &= \chi_0 \left\{ \frac{\omega_{13A}^2}{\omega_{13A}^2 - \omega^2} - \frac{\omega^2 \gamma^2 H_e^2 H_{A3}^2 l_z^4 / \tilde{H}_{13}^2}{(\omega_{13A}^2 - \omega^2)(\omega_{13O}^2 - \omega^2)} \right\}, \\ \chi_{xx}(\omega) &= i\tilde{\chi}_0 \left\{ \frac{\omega_{24A}^2}{\omega_{24A}^2 - \omega^2} - \frac{\omega^2 \gamma^2 H_e^2 H_{A3}^2 l_z^4 / \tilde{H}_{24}^2}{(\omega_{24A}^2 - \omega^2)(\omega_{24O}^2 - \omega^2)} \right\}, \end{aligned} \quad (37)$$

$$\chi_{zz}(\omega) = \chi_0 \gamma^2 (H + H_{D2} l_z)^2$$

$$\left\{ \frac{1}{\omega_{24A}^2 - \omega^2} - \frac{H_e^2 H_{A3}^2 l_z^4 / \tilde{H}_{24}^2}{(\omega_{24A}^2 - \omega^2)(\omega_{24O}^2 - \omega^2)} \right\},$$

$$\begin{aligned} \chi_{zx}^*(\omega) &= -\chi_{xz}(\omega) = i\omega\chi_0\gamma(H + H_{D2}l_z) \\ &\times \left\{ \frac{1}{\omega_{24A}^2 - \omega^2} - \frac{H_e^2 H_{A3}^2 l_z^4 / \tilde{H}_{24}^2}{(\omega_{24A}^2 - \omega^2)(\omega_{24O}^2 - \omega^2)} \right\}. \end{aligned}$$

Here

$$\begin{aligned} \tilde{H}_{13,24}^2 &= (H + H_{D2}l_z) [H + (2H_{D1} + H_{D2})l_z] \\ &+ 2H_e(\pm 2H'_e + H_{A2} - H_{A1})l_z \end{aligned}$$

and the plus sign is taken for \tilde{H}_{13} , the minus sign for \tilde{H}_{24} .

Expressions (37) imply that the components of the rf magnetic susceptibility tensor in the Γ_3 phase have residues at the exchange frequencies. These residues are proportional to the monoclinic anisotropy H_{A3} . In the Γ_4 phase the residues at the optical modes are also proportional to the parameter H_{A3} , which has also determined the degree to which the magnetic structure of the system is canted in this phase. For this reason one could get the impression that the intensity of the absorption at the optical frequencies is determined by the degree of canting of the structure. However, as we have mentioned, the system is collinear in the Γ_3 phase (the antiferromagnetism vector \mathbf{L}_i and the ferromagnetism vector \mathbf{F}_i of the layers are mutually collinear). Nevertheless, the corresponding residues at the optical modes are nonzero. Thus the intensity of the absorption at optical modes is determined not by the degree of canting of the system but by the magnitude of the effective anisotropy fields which cause the many-sublattice structure of the system to be manifested in the dynamics. In some cases, such as the Γ_4 phase, for example, the anisotropy causes the many-sublattice nature of the system to be manifested even in the statics, giving rise to a canting of its magnetic moments. In other cases, such as the Γ_3 phase, for example, it is manifested only in the dynamics. However, for the intensity of the absorption by optical modes the dynamic many-sublattice nature always has priority over the static.

The static susceptibility of the system can be obtained

from (37) by taking the limit $\omega \rightarrow 0$, $H \rightarrow H_c$. As a result we find

$$\chi_{yy}(0) = \chi_{xx}(0) = \chi_0, \quad (38)$$

$$\chi_{zz}(0) = \chi_0 \gamma^2 (H + H_{D2} l_z) (\omega_{24A}^2 - H_e^2 H_{A3}^2 l_z^4 / H_{24}^2 \omega_{24A}^2 \omega_{24O}^2).$$

The component $\chi_{zz}(0)$ has a nonzero residue at the exchange frequency. The reason for this is that for $\mathbf{h} \perp \mathbf{z}$ the system acquires an admixture of the Γ_4 phase, which has a four-sublattice configuration of the magnetic moments even in the statics, i.e., the external field along the z axis causes not only a bending of the magnetic sublattices toward this axis but also a rotation of these sublattices.

The Γ_{34} and γ_{13} phases

A detailed theoretical calculation of the rf properties of the system and a comparison of the results of this calculation with experiment in the Γ_{34} and Γ_{13} phases will be the subject of a separate paper. Here we shall give only a qualitative analysis of the experimental behavior of the optical and acoustic modes of the AFMR in these phases.

In the Γ_{34} phase ($0 < H < H_{sf}$) the configuration of the magnetic moments of the system is invariant with respect to the operations E and C'_{2x} which generate the magnetic class $C_2(C_1)$. Because the only unitary operation in the Γ_{34} phase is the identity operation, all the AFMR modes have the same symmetry. Therefore, the frequencies ω_{1234O} and ω_{1234A} should repel each other. However, no repulsion of the branches is observed within the experimental error. The reasons for this are as follows.

It can be shown that for $H_D = 0$ the magnetic symmetry of the system is effectively increased and becomes equivalent to the symmetry of a structure of the plane cross type, considered in Ref. 3. It follows that in this approximation the optical and acoustic modes do not interact with each other. On the other hand, even for nonzero H_D but $\mathbf{H} = 0$ the vibrations ω_{1234O} and ω_{1234A} have different symmetries and, here too, do not interact. Since an H_{D1} of 1.7 kOe in PDAMnCl₄ causes a slight canting of the magnetic configuration ($H_{D1}/H_e \approx 0.001$) and since the external magnetic field at which the crossing of the branches is observed (see Fig. 4) cannot substantially alter the ground state of this antiferromagnet, it can be shown that the value of the repulsion should be of the order of $HH_{D1}/H_e \approx 0.01$ kOe. Such a value is difficult to observe experimentally because of the masking effect of the finite AFMR linewidth.

If the Γ_{13} phase (field region $H_{sf} < H < H_c$) the magnetic configuration of the system is described by the class $C_2(C_2)$. The corresponding oscillatory modes transform according to the two representations Γ_{13} and Γ_{24} . A symmetry analysis shows (see the third row in Table III) that the frequencies $\omega_{13O,A}$ are excited by an rf field $\mathbf{h} \parallel \mathbf{y}$ and the frequencies $\omega_{24O,A}$ are excited by an rf field $\mathbf{h} \perp \mathbf{y}$.

Experimentally this phase exhibits a strong interaction of the optical and acoustic modes which transform according to the representation Γ_{24} (see Fig. 4). It can be shown that the interaction of the ω_{24O} and ω_{24A} branches does not vanish even for $H_D = 0$, and the strength of the interaction is determined by \mathbf{H} and H_A .

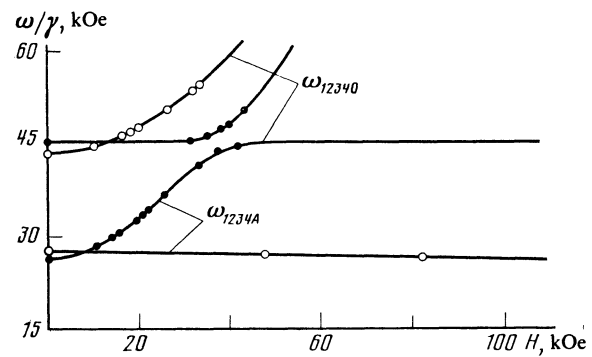


FIG. 6. Frequency-field diagram of the AFMR for $\mathbf{H} \parallel \mathbf{x}$. The solid lines are drawn through the experimental points.

The presence of an interaction of the optical and acoustic modes and the formation of coupled vibrations with different types of precession were first detected in Ref. 6. It was also shown there that the coupling of the optical and acoustic modes in low-dimensional many-sublattice magnets should be observed in fields $\sim (H_e H_A)^{1/2}$ because of the substantial lowering of the optical mode frequencies in systems of this kind. Three-dimensional magnets can exhibit similar effects for $H \sim H_e$, as has been observed⁵ in AFMR experiments on $\text{CuCl}_2 \cdot 2\text{H}_2\text{O}$.

5. $\mathbf{H} \parallel \mathbf{x}$

An external magnetic field directed along the x axis induces a magnetic moment F_x parallel to this axis. As we see from Table II, the magnetic class in this case is $C_1(C_1)$, and a mixed magnetic configuration containing all the components of vectors (1) is realized.

The experimental frequency-field curves of the AFMR for $\mathbf{H} \parallel \mathbf{x}$ are given in Fig. 6. Being of the same symmetry, the modes interact. In weak fields the interaction of the optical modes with each other and the interaction of the acoustic modes with each other are determined by the small parameter HH_D/H_e and are therefore not observed in experiment. In fields $H \approx 40$ kOe the nature of the interaction of the optical and acoustic modes is basically analogous to that of the interaction of the optical and acoustic modes in the Γ_{13} phase ($\mathbf{H} \parallel \mathbf{y}$), and therefore the repulsion of the branches is of the same order of magnitude (see Fig. 6).

V. CONCLUSION

We have shown in this paper that the specific features of two-dimensional four-sublattice magnets are manifested rather clearly in PDAMnCl₄. We have made the first experimental and theoretical study of the case of a low-dimensional relativistically canted magnetic structure, which has unusual rf and static properties.

We have shown that the AFMR spectrum of a four-sublattice low-dimensional antiferromagnet cannot in principle be described in the two-sublattice mode and that in the case of low-dimensional antiferromagnets, unlike the three-dimensional case, the formal division between acoustic and exchange branches of the AFMR spectrum vanishes because

of the strong depression of the optical mode frequencies.

By studying all the branches of the AFMR spectrum we were able to reconstruct the magnetic structure of PDAMnCl₄ without using complicated neutron diffraction methods and to determine the constants of the thermodynamic potential.

We note that our analysis of the rf properties of PDAMnCl₄ has enabled us to describe in this particular case the behavior of the optical and acoustic modes as a function of the field and of the parameters of the system and to give the values of their intensities, which turn out to be substantially dependent on both the ground-state magnetic configuration of the system and on the excitation conditions. This indicates that the quantitative description of the behavior of the system is not amenable to simple criteria. Qualitatively, the question of the interaction between different modes and the possibility of their excitation by a magnetic field has been resolved unambiguously on the basis of the symmetry methods developed in Ref. 11.

The presence of additional branches of the AFMR should be manifested in the thermodynamics of the system and in the temperature dependence of the magnetization and of the gap in the spin-wave spectrum. We propose to study these questions both experimentally and theoretically in the future.

For the example of the spin-flop transition in PDAMnCl₄ we have demonstrated the specifics of the spin-reorientation transitions in low-dimensional magnets. More-detailed studies of the spin-flop transition in this compound are also of interest, especially a study of the character of the transition, the critical angles of inclination of the magnetic field, the angular dependence of the AFMR spectra near the transition field, etc.

In closing we express our gratitude to V. G. Bar'yakhtar

for constructive comments in the course of this study and to V. V. Eremenko for a fruitful discussion.

¹¹According to the x-ray diffraction data the compounds of this family with different magnetic ions Mn²⁺ or Cu²⁺ have the same symmetry for a given n (for $n = 2, 4$, and 5).

²¹The value of $\chi_{zz}(0)$ can also be obtained directly by differentiating expression (7) for m_z with respect to the field and then using the equation of the ground state (8).

¹R. J. Joenk, Phys. Rev. **126**, 565 (1962).

²G. F. Herrmann, Phys. Rev. **133**, A1334 (1964).

³Yu. G. Pashkevich, V. L. Sobolev, and V. T. Telepa, Fiz. Nizk. Temp. **8**, 705 (1982) [Sov. J. Low Temp. Phys. **8**, 351 (1982)].

⁴V. V. Eremenko, V. M. Naumenko, Yu. G. Pashkevich, and V. V. Pishko, Pis'ma Zh. Eksp. Teor. Fiz. **38**, 97 (1983) [JETP Lett. **38**, 112 (1983)].

⁵V. G. Bar'yakhtar, V. V. Eremenko, V. M. Naumenko, *et al.*, Zh. Eksp. Teor. Fiz. **88**, 1382 (1985) [Sov. Phys. JETP **61**, 823 (1985)].

⁶A. A. Stepanov, M. I. Kobets and A. I. Zvyagin, Fiz. Nizk. Temp. **9**, 764 (1983) [Sov. J. Low Temp. Phys. **9**, 391 (1983)].

⁷H. Van Kanel, Physica B **96**, 167 (1979).

⁸R. D. Willet and E. F. Ridet, Chem. Phys. **27**, 112 (1975).

⁹D. B. Losee, K. I. McGregor, W. E. Estes, and W. E. Hatfield, Phys. Rev. B **19**, 4100 (1976).

¹⁰V. A. L'vov and D. A. Yablonskiĭ, Fiz. Nizk. Temp. **8**, 951 (1982) [Sov. J. Low Temp. Phys. **8**, 479 (1982)].

¹¹V. G. Bar'yakhtar, I. M. Vitebskiĭ, and D. A. Yablonskiĭ, Zh. Eksp. Teor. Fiz. **76**, 1381 (1979) [Sov. Phys. JETP **49**, 703 (1979)]; D. A. Yablonskiĭ, Author's Abstract of Candidate's Dissertation, Donetsk (1980).

¹²E. P. Wigner, *Theory of Groups and its Application to the Quantum Mechanics of Atomic Spectra*, Academic Press, New York (1959).

¹³V. G. Bar'yakhtar, A. E. Borovik, and V. A. Popov, Zh. Eksp. Teor. Fiz. **62**, 2233 (1972) [Sov. Phys. JETP **35**, 1169 (1972)].

¹⁴A. M. Kosevich, B. A. Ivanov, and A. S. Kovalev, Nelineĭnye Volny Namagnichennosti. Dinamicheskie i topologicheskie Solitony [Nonlinear Magnetization Waves. Dynamic and Topological Solitons], Naukova Dumka, Kiev (1983), p. 190.

¹⁵A. P. Levanyuk and A. A. Sobyenin, Zh. Eksp. Teor. Fiz. **53**, 1024 (1967) [Sov. Phys. JETP **26**, 612 (1968)].

¹⁶V. G. Bar'yakhtar, I. M. Vitebskiĭ, Yu. G. Pashkevich, *et al.*, Zh. Eksp. Teor. Fiz. **87**, 1028 (1984) [Sov. Phys. JETP **60**, 587 (1984)].

Translated by Steve Torstveit